Drug–Biomolecule Interactions: Bioelectrometric Study of the Mechanism of Carbachol Interactions with the Cornea and Its Relation to Miotic Activity

VICTOR F. SMOLEN ˣ, CHUI S. PARK, and EDWARD J. WILLIAMS

Abstract □ The augmentation of carbachol miotic activity attributable to enhanced transcorneal absorption, which results from the action of cationic adjuvants included in ophthalmic vehicles, suggested a study of carbachol–corneal tissue interaction as a further step toward understanding the phenomenon. The present study was performed *in vivo* using an innocuous electrometric technique. A fixed charge density of the corneal epithelial surface *versus* carbachol concentration profile was obtained from the electrometric results; it revealed three distinct concentration regions defined by precipitous decreases of fixed charge over extremely small concentration ranges. This anomalous behavior is attributed to cooperative alterations in the binding affinities of fixed anionic sites on the tissue surface, which result in an all-or-none release of protons and/or other microcations. The unmasked anionic sites become reoccupied with carbachol except in the last region where the reoccupation by carbachol is competitive with other cations in the solution in contact with the surface. This behavior, postulated on the basis of the construction of a carbachol–tissue binding isotherm from which thermodynamic interaction affinities were computed, was corroborated by the observed dependency of the duration of miotic activity on carbachol concentration. Allosteric interactions between anionic binding sites, which are mediated through electron inductive and electrostatic field effects and likely involve a cooperative alteration in tissue water structure, are implicated as underlying the observed phenomena.

Keyphrases □ Carbachol—interactions with cornea, relation to miotic activity, mechanism, bioelectrometry □ Ophthalmic solutions—carbachol interactions with cornea, relation to miotic activity, mechanism, bioelectrometry □ Bioavailability—ophthalmic carbachol, interactions with cornea, relation to miotic activity, mechanism, bioelectrometry □ Drug–biomolecule interactions—mechanism of carbachol interactions with cornea, relation to miotic activity, bioelectrometry □ Interactions—drugs with biomolecules, symposium

The first report (1) in the present series described the considerable augmentation of carbachol miotic activity resulting from the inclusion of benzalkonium chloride, a cationic surfactant, or a dextran (DEAE), a cationic polyelectrolyte, in an ophthalmic vehicle. This phenomenon, first reported for benzalkonium chloride (2), was discussed briefly and attributed to a modulation of carbachol–tissue interaction by the cationic adjuvants resulting in a promoted biophasic availability of the drug. The adjuvants appear to be selective in their enhancement of the transcorneal availability of the drug to its site of miotic action without concomitantly increasing systemic absorption.

The present report describes details of a bioelectrometric investigation of the interaction of carbachol with the corneal epithelial surface of rabbits. The *in vivo* bioelectrometric technique (3–8) is unique in its ability to provide data that permit characterization of drug–tissue interactions in terms of kinetic and thermodynamic parameters (7, 10–13) under physiological, product-use, conditions. The technique often provides a unique means for obtaining such information.

EXPERIMENTAL

Materials—All reagents were analytical grade except for the carbachol[1] USP (carbamylcholine chloride). Pentobarbital sodium[2] and lidocaine hydrochloride[3] were used as general and local anesthetics, respectively. Filter paper wick material[4] was used for measuring electrical potentials[5]. Fiber junction, miniature, saturated calomel electrodes[6] were attached using Tygon rubber sleeves to the filter paper wicks, which were used for corneal measurements; a glass-sleeve-type electrode[6] was used as the reference electrode immersed in the 0.15 *M* NaCl reference solution. A micromanipulator[7] was used to apply the wicks to the corneal surface. The liquid junction potential measuring apparatus was described previously (8).

The composition of the carbachol-free buffer solutions employed in the pH titration experiments was reported earlier (5). Carbachol solutions[8] were prepared by the addition of carbachol to pH 6.95 phosphate buffer solutions. Conductance measurements were performed with a conductivity bridge[9]. The animals used were approximately 2-month-old male New Zealand white rabbits, 2.0–2.5 kg.

Miotic Response Monitoring—The details of the administration of ophthalmic drug solutions into the eyes of the rabbits and the recording of drug-induced time variations in the pupillary diameter were reported previously (1, 12–14).

Bioelectrometric Methodology—The previously described dilution potential method (3–5, 15), as contrasted to an equilibrium method or the dilution-potential–time extrapolation method (11), was utilized to determine the dependency of the fixed charge density of the corneal surface on the composition of applied experimental solutions. The fixed charge density arises from the dissociation of ionogenic groups covalently bonded to or sorbed onto the biocolloids constituting the tissue surface (14).

The net density of fixed charge is generally a sensitive function of the composition of the solution contacting the tissue. The verity of observed dilution-potential measurements in reflecting the fixed charge density has been confirmed by direct experimentation (8). The often direct relationships between observed changes in fixed charge density and the extent of solute binding to tissue surfaces have also been demonstrated (6, 7, 11).

Except for some minor modifications, the employed procedure is similar to the technique described earlier for the interaction of procaine hydrochloride with the cornea of guinea pigs (3). The experimental arrangement for the present study with rabbits is illustrated in Fig. 1. The rabbits were immobilized by slowly infusing a

[1] Alcon Labs., Inc., Fort Worth, Tex.
[2] Nembutal Sodium, Abbott Laboratories.
[3] Xylocaine Hydrochloride, Astra Pharmaceutical Co.
[4] Beckman, Catalog No. 320046.
[5] Sargent SR recorder.
[6] Beckman.
[7] Model UD-1, Narishige Scientific Instrument Laboratory, Tokyo, Japan.
[8] The pH of all solutions was measured with an Orion model 801 digital pH meter.
[9] Serfass.

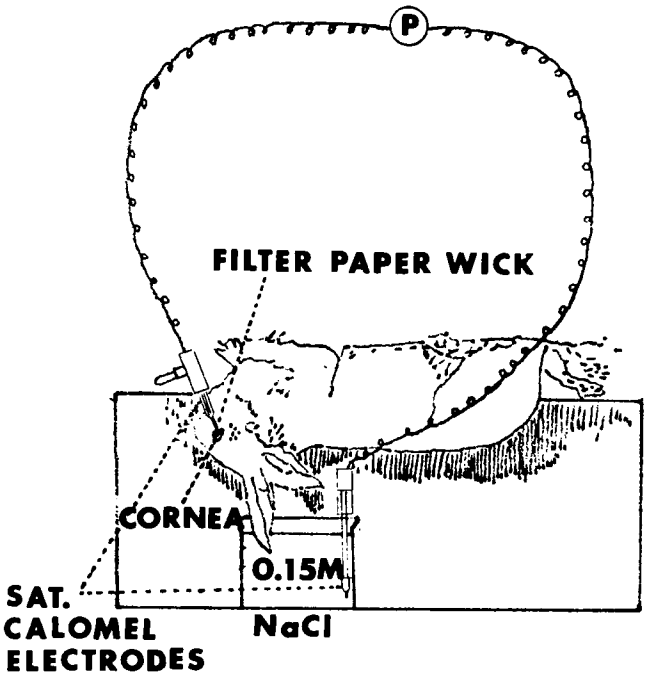

Figure 1—*Experimental arrangement for the bioelectrometric determination of the fixed charge density of the rabbit cornea.*

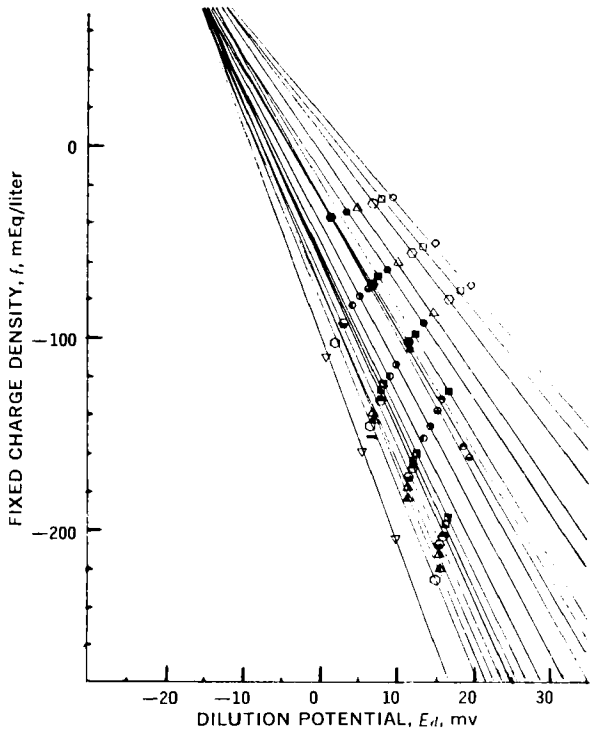

Figure 2—*Calibration plots for the transformation of experimentally observed dilution potential values into corresponding fixed charge densities. The curves relate to:* (○) *pH 6.95 buffer without carbachol and the same buffer containing varying carbachol concentrations,* i.e., (□) *0.0055*M, (○) *0.0137* M, (△) *0.0274* M, (●) *0.038* M, (■) *0.049* M, (◉) *0.055* M, (◓) *0.060* M, (◒) *0.066* M, (◑), *0.077* M, (◐) *0.088* M, (◔) *0.099* M, (◩) *0.104* M, (◓) *0.110* M, (◒) *0.115* M, (▲) *0.121* M, (◭) *0.129* M, (○) *0.137* M, *and* (▽) *0.164* M.

dilute solution (0.6% w/v) of pentobarbital sodium into a marginal ear vein. The required dose varied between 30 and 40 mg/kg.

Retrobulbar injection of 1 ml of a 1% (w/v) solution of lidocaine hydrochloride was administered to the anesthetized rabbits to diminish blinking and lacrimation and to permit freer access of the filter paper wicks to the cornea by causing the eye to protrude slightly. The retrobulbar injection of lidocaine did not alter the results of the corneal electrometric measurements. Each rabbit was allowed a minimum recovery period of 1 week between successive experiments in which the right and left eyes were used alternately.

As shown in Fig. 1, the rabbit's ear was depilated and immersed in a 0.15 *M* NaCl solution along with the saturated calomel reference electrode. This rabbit's ear served as a reference surface, and it was not disturbed during an experimental run. The dilution potential procedure for a particular solution consisted of thoroughly rinsing the cornea with buffer, blotting off the excess solution with cotton swabs and filter paper wicks, and contacting the center of the cornea with a filter paper wick which had been wetted with the experimental solution and attached to the fiber junction of an electrode.

Following contact of the solution-wetted wick with the cornea, a potential, E_1, was recorded until it became constant. For an eye thoroughly rinsed with buffer just prior to the measurement, constancy in E_1 was achieved almost immediately. Without further treatment of the eye, a second slightly smaller filter paper wick wetted with a 10-fold dilution of the experimental solution and attached to a second electrode precisely matched to the first (*i.e.*, asymmetry potentials measured between the electrodes with both immersed in 0.15 *M* NaCl solution were less than 0.1 mv) was placed within the area of the cornea covered during the measurement of E_1. A second potential, E_2, was recorded immediately upon contact of the dilute solution with the corneal surface. Each measurement of E_1 and E_2 was replicated with the same solution and its dilution; this procedure was repeated for all experimental solutions in a series.

Extreme care was exercised in the positioning of the solution-wetted wicks on the cornea and also in the swabbing of excess solution from the eye so as not to abrade the cornea or touch surrounding tissues. In each measurement, the micromanipulator was used to lower the wick slowly to the center of the cornea until electrical contact was made by pendular drops of solution adhering to the end of the wick rather than by the wick itself. Consistent adherence to this technique prevented abrasion of the cornea as well as position and movement effects on corneal potentials (16–18); such effects did not present a problem in the present study. The filter paper wick itself must not possess a fixed charge density which varies with the composition of its imbibed solutions since this can cause a considerable error in the results.

Whether a particular wick material is satisfactory or not can be determined from liquid junction potentials obtained with a strip of the wick material serving as a bridge between the experimental solutions and their 10-fold dilutions. The procedure for this determination is identical to that previously described for a strip of cation-exchange membrane material (8).

Conversion of Measured Dilution Potentials into Fixed Charge Densities—Theoretical expressions relating the difference in the two measured potentials, $(E_2 - E_1)$, termed the dilution potential, E_d, to the fixed charge density of the tissue surface for an applied experimental solution were presented previously (3, 7, 15). The equations are most conveniently solved graphically or through the construction of alignment charts.

Figure 2 presents the calibration curves used to relate experimental E_d values to corresponding values of fixed charge density for each pH 6.95 carbachol solution–10-fold dilution pair used. The curves are linear over the E_d range of interest; the slopes of the curves vary with the content of carbachol contained in their corresponding solutions. The limiting ionic conductance, λ_0, of the carbamylcholine cation required for construction of the calibration curves was determined both by conductance and liquid junction potential measurements to yield a nearly identical average value of 38.9 ohms^{-1} at 25° for carbachol concentrations ranging from 5.5 to 274 m*M* in the pH 6.95 buffer. Experimental methods for measuring λ_0 were described previously (8).

The verity of the application of the theoretical expressions for relating fixed charge density values to observed dilution potentials, *via* the calibration curves in Fig. 2, was confirmed by liquid junction potential measurements (3, 5). Fixed charge densities corresponding to dilution potentials measured with buffered solutions of varying pH, but not containing carbachol, were obtained using a previously reported alignment chart (5).

Relation of Dilution Potential Method to Other Corneal

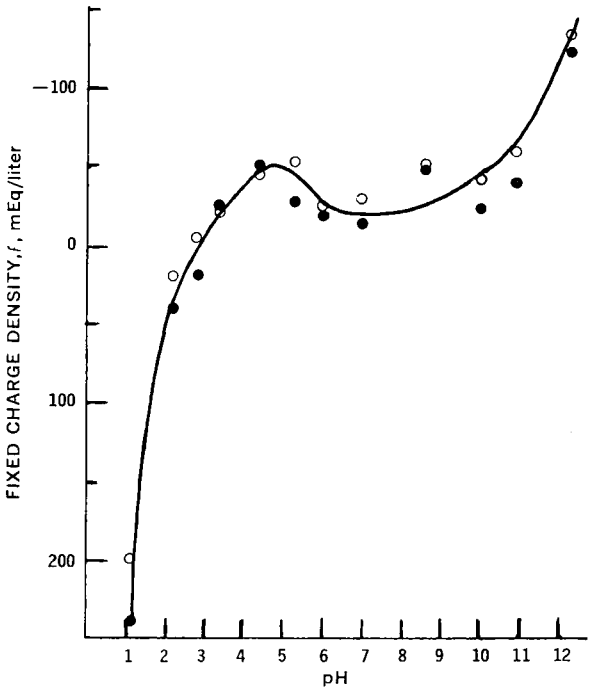

Figure 3—*Bioelectrometric pH titration curve of the corneal surface of rabbits. Key:* O, *forward titration; and* ●, *reverse titration.*

Potential Recording Techniques—In contrast to the transmembrane type of potentials recorded on the cornea by various other investigators (16–19), the dilution potentials determined in the present study are liquid junction potentials that develop across the interphase formed immediately upon contact between the experimental solution, with which the corneal surface has been allowed to equilibrate, and the 10-fold dilution of the same solution.

The E_d values depend only upon the composition of the solutions and the fixed charge characteristics of the tissue surface existing under the conditions of their application. Therefore, the E_d potentials obtained cannot be directly compared to corneal potentials reported by other investigators using other techniques which provide results that cannot be interpreted as readily (15–18). Caution is particularly required in comparing *in vivo* corneal potentials with results recorded from excised corneas. When using the dilution potential methods, differences become clearly evident. Details of the comparison of *in vivo* to *in vitro* electrometric results will be presented subsequently.

RESULTS AND DISCUSSION

pH Titration Curves of Corneal Surface—Figure 3 illustrates how the fixed charge density of the corneal surface varies with the pH of the applied solution; numerical values are presented in Table I. The plot in Fig. 3 is analogous to pH titration curves of amphoteric macromolecules in that it also describes proton ionization. It differs somewhat in that the shape of the curve also reflects the influence of other solutes in the experimental solutions applied to the tissue surface.

The variation in fixed charge density of the surface with increasing pH derives from the dissociation of protons from chemical groups covalently bonded to protein, nucleic acid, phospholipid, and mucopolysaccharide tissue constituents of the corneal surface. The variation is also affected by the binding of other ionic or uncharged solutes (present in the milieu of the tissue surface) to charged or neutral surface sites (3, 7, 15). The observed density of fixed charge at any time is a consequence of the interacting state of these biocolloids as a whole and is quite sensitive to the composition of the applied solutions.

Previous results from this laboratory describing the effects of surfactants (7, 15), hexachlorophene (5–7), and carcinogenic and inactive hydrocarbons (4) with human epidermis, as well as the interaction of procaine with the corneal surface (3), have been reported. Direct correlations between tissue binding (5, 7) or pharmacological activity (3) of the tissue-interacting solutes and observed changes in fixed charge density have been demonstrated.

Table I—Fixed Charge Density Values for the Forward (Low to High pH) and Reverse (High to Low pH) Hydrogen-Ion Titration of the Corneal Surface of Rabbits

pH	E_d, mv		Fixed Charge Density, f, ± SD, mEq/liter[a]	
	Forward	Reverse	Forward Titration	Backward Titration
1.12	−1	−8	+200 ± 46	+240 ± 30
2.20	−9	−14	+20 ± 10	+40
2.82	−9	−14	−5 ± 15	+20
3.39	−7	−6	−23 ± 3	−25
4.40	−2	−1	−44 ± 24	−51 ± 31
5.33	+6	+1	−53 ± 39	−28 ± 19
5.99	+8	+6	−24 ± 13	−19 ± 23
6.95	+9	+6	−29 ± 5	−14 ± 15
8.60	+5	+4	−51 ± 22	−49 ± 22
10.07	−3	−7	−42 ± 9	−23 ± 16
10.91	−2	−5	−60	−40
12.30	−8	−10	−135	−125

[a] The values are averages of a minimum of eight replications except for single determinations which are listed without standard deviations.

The fixed charge densities plotted as a pH titration curve in Fig. 3 appear to be independent of whether the measurements were initiated at low or high pH; a forward titration curve (pH 1.12–12.30) was not statistically different from the reverse curve (pH 12.30–1.12) at a $p \leq 0.05$ confidence level as determined using a paired t test. However, an opacity of the cornea with an accompanying red coloration and mucous lacrimation usually appeared at low (1.12–3.39) and at high (10.07–12.30) pH during the electrometric titration. It has been reported that the cornea can be severely damaged at pH 11 (21).

In view of these changes in the cornea observed at the extremes of pH, the apparent nonhysteretic nature of the forward and reverse titration curves was unexpected; the fixed charge density in the past has been shown to be a sensitive means of detecting changes in the structure and properties of tissue surfaces. The apparent failure of the bioelectrometric results to exhibit hysteresis in the acid–base binding characteristics of the cornea may be attributed to the following causes:

1. Whatever changes do occur are reversible.
2. Irreversible changes occur at depths within the cornea below those for which the electrometric results reflect the state of tissue colloids; for epidermis, the depth is approximately 3–4 μm (6, 7). Although a similar determination was not performed for the cornea, it may be assumed that the stratum corneum of the epidermis is appreciably more porous than the unkeratinized corneal epithelium and that the corneal tissue depth represented electrometrically in the present case is much less than that estimated for epidermis.
3. The damage to the corneal epithelium is the same for both acidic and alkaline pH extremes. The difference in the fixed charge density at pH 6.95, given in Table I as 29 ± 5 mEq/liter, compared to the value of 70 ± 13 mEq/liter (Table II), which was observed for corneas not previously treated with solutions other than pH 6.95, supports this conclusion.

When referring to Fig. 3, it is apparent that the isoelectric point of the corneal surface is in the vicinity of pH 3.0. At the isoelectric pH, the number of basic, fixed cationic groups exactly balances the number of acidic, fixed anionic groups titrating below the isoelectric point. The relatively low isoelectric point of the corneal surface is largely attributable to the presence of sulfate groups on its mucopolysaccharide constituents, although some carboxyl groups are also titratable below pH 3.0 (22).

Since the lowest pH at which cationic groups on the surface start to deprotonate is above pH 5 and the anionogenic groups all may be assumed to be essentially protonated at pH 1.12 (23), the observed difference in fixed charge density, ≃200 mEq/liter, which is the difference between the charge density at pH 1.12 and that at the isoelectric pH, is assumed to represent the density of fixed cationic sites on the tissue surface.

Table II—Dependence of *In Vivo* Corneal Surface Fixed Charge Density, *f*, on Carbachol Concentration in pH 6.95 Phosphate Buffer as Determined Electrometrically

Carbachol Solution Molarity	Carbachol Molarity at Corneal Surface, $r^Z M$[a]	E_d,[b] mv	$f \pm SD$, mEq/liter	Δf[c], mEq/liter
0 (buffer)	0	+19	−70 ± 13	0
0.0055	0.0069	+16	−67 ± 14	+3
0.0137	0.017	+14	−64 ± 12	+6
0.0274	0.032	+10	−58 ± 9	+12
0.038	0.044	+6	−50 ± 13	+20
0.049	0.054	+3	−37 ± 11	+30
0.055	0.058	0	−25 ± 18	+45
0.060		+5	−66 ± 17	+4
0.066	0.088	+12	−117 ± 12	−47
0.077	0.090	+4	−67 ± 19	+3
0.088	0.098	0	−50 ± 16	+20
0.099	0.108	−2	−42 ± 21	+28
0.104	0.100	−3	−34 ± 26	+36
0.110	0.111	−7	−1 ± 33	+69
0.115		−2	−54 ± 24	+16
0.121	0.125	+4	−109 ± 20	−39
0.129	0.145	−1	−65 ± 28	+5
0.137	0.153	−2	−61 ± 35	+9
0.164	0.173	−6	−37 ± 29	+33

[a] $Z = 1$ for carbamylcholine cation. [b] Average values from 28 determinations. [c] Δf = *f* (carbachol) − *f* (buffer).

It can be seen in Fig. 3 that the net fixed charge density is anionic above pH 3.0, passing through a shallow minimum at approximately pH 6.5. The apparent minimum in the curve may at first appear quite anomalous since it indicates that an increase in the cationic charge density of the surface occurs with increasing pH over the 4.5–6.5 pH range whereas deprotonation of the surface, as may ordinarily be expected to occur with increasing pH, causes the surface charge density to decrease. This same behavior has also been observed in this laboratory with titration curves obtained *in vivo* on rabbit intestinal mucosa and frog skin. Less physiologically active tissue surfaces such as epidermis and connective tissue, which do not actively transport ions across their single or multicellular barriers, exhibit this effect to a minor degree or not at all (5, 7, 15).

Presently unpublished results of additional studies with frog skin and the mucosal surface of the lower third of the rabbit duodenum have shown that the anomaly in the titration curves of these tissue surfaces is due to the binding of Na^+ ions, which occurs in increasingly larger concentrations in the higher pH buffer solutions, to the tissue surfaces at a rate exceeding the rate of deprotonation of fixed anionogenic surface sites. Experiments at fixed pH have revealed a similar U-shaped response in anionic fixed charge density to increasing concentrations of Na^+ ions, indicating that the Na^+ ions themselves can trigger their own release from tissue-binding sites.

A mechanism involving "cardinal" Na^+ binding sites, whose extent of occupation governs the affinity of "gangs" of other Na^+ binding sites by an allosteric, electron-inductive mechanism similar to that previously postulated (4–6, 15, 24–27) is hypothesized as being operative in this phenomenon and active Na^+ transport (25). A related behavior is demonstrated by the results shown here for carbachol.

Carbachol Interaction with Corneal Surface—Figure 4 contains plots of carbachol-induced changes in the fixed charge density of the rabbit cornea as a function of carbachol concentration; each point is the average of at least 28 replications performed with different rabbits. The data are summarized in Table II.

It is apparent from inspection of Fig. 4 that increases in the cationic fixed charge density of the surface with increasing carbachol concentration occur in three discrete concentration ranges. Each range is well delineated by a precipitous drop in the density of the fixed positive surface charge. Therefore, an unexpected phenomenon of a cationic sorptate interacting with an anionic sorbent to render it more anionic over a very small range of concentration is observed. In view of related phenomena reported from this laboratory, *e.g.*, hexachlorophene anion binding to a negatively charged epidermal surface which *reduces* its net anionic charge density (5, 6) and similar results from other laboratories (28), these apparently paradoxical carbachol effects on the cornea do not appear quite as unusual.

As previously reported (5), the effects of hexachlorophene anions on the fixed charge density of the epidermal colloids at pH 10 were attributed to the operation of electrostatic field effects in conjunction with inductive delocalization of electrons emanating from peptide nitrogen binding sites to increase the acid pK's of vicinal ionogenic protein side groups. The shift in pK results in an uptake of protons, as well as probably other mobile microcations, from the solution and produces a diminution in anionic fixed charge density.

A similar mechanism was postulated as being responsible for repression of the ionization of fixed anionogenic sites on skin that was observed to be induced by sodium lauryl sulfate (7). Predictive evidence for such hypotheses was presented in a later paper (20) in the form of a hexachlorophene anion-induced inversion of the specific electrical response behavior of the epidermal surface to Na^+ and K^+ ions. The present observed behavior of the fixed charge density of the corneal surface in response to carbachol interaction is most closely analogous to the influence of unionized hexachlorophene on the skin at lower pH (5) or of 3-methylcholanthrene (4); both agents manifest their effects in an increase in the net anionic fixed charge density that can be attributed to an inductive withdrawal of electrons from vicinal ionogenic sites, resulting either in their deprotonation or to their dissociation of other possible microcations with which the sites might also be occupied (6). Similar allosteric mechanisms have been postulated (24, 27, 29–31).

The ability of electron-inductive effects to be transmitted for appreciable distances through biopolymers such as proteins and nucleic acids possessing semiconductive properties has been convincingly postulated (29, 32, 33). The mechanisms postulated for the presently observed phenomena are also involved in solute-induced changes in the pK's of titratable groups of wool and soluble proteins and are manifested in lateral shifts in hydrogen bonding curves (34–36) as well as, for example, drug and calcium-ion-induced lateral shifts in the intracellular Na^+ and K^+ binding isotherms of muscle (37, 38).

With these principles in mind, the initial increases in cationic fixed charge density in each discrete carbachol concentration range (Fig. 4) can be attributed to direct electrostatic binding of carbachol cations to fixed anionic sites, similar to that demonstrated for various different cations binding to wool (39), plasma proteins (40), the epidermis (4, 41), and the cornea (3). In each

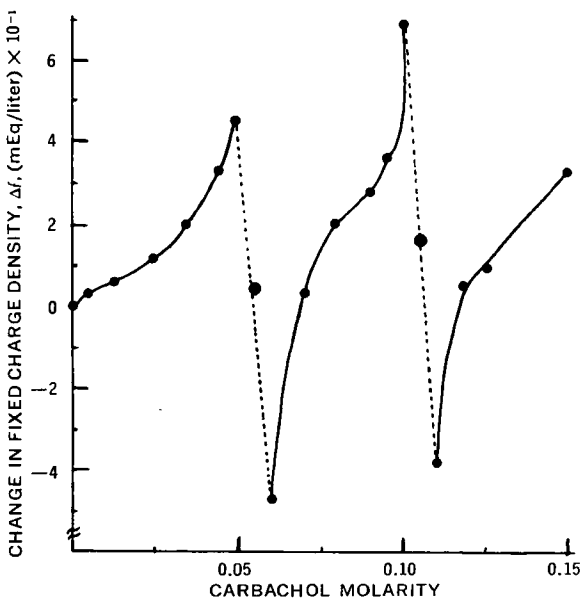

Figure 4—*Dependency of carbachol-induced changes in the fixed charge density of the corneal surface. The ordinal values are changes relative to the fixed charge density at pH 6.95 in the absence of carbachol. Each value is the average of 28 determinations performed on different rabbits.*

case, a long-range coulombic attraction has been postulated to be responsible for a sufficiently close approach of cationic solutes to anionic binding sites so as to cause electrostatic salt binding to occur and to be reinforced by secondary, short-range van der Waals forces.

The abrupt appearance of new, fixed, anionic tissue surface sites, which is observed when carbachol interacts with the cornea, may be attributed to a triggering of a cooperative (22, 29), inductively implemented, reduction in the electron charge densities of anionic sites transiently occupied by cations. These sites are vicinal to carbachol binding sites. The cooperative nature of the phenomenon may be compared to the analogous mechanism by which cationic surface-active agents denature proteins (32, 42). The carbachol-induced alterations of neighboring sites can be postulated to occur by electron withdrawal, resulting in a reduced affinity (decreased acidic pK) for binding protons and presumably other cations and depending on such factors as their hydrated diameters and relative concentrations (24, 43). This reduced binding affinity allows the release of the cations into the milieu and results in an abrupt increase in the negative fixed charge density of the tissue surface. The anionic sites vacated by the released cations become available for binding carbachol, with the process again being repeated when a sufficient density of these interaction sites becomes occupied to trigger another all-or-none type of cooperative transformation resulting in the release of additional cations.

Considering that *(a)* a carbachol-induced electron withdrawal from neighboring anionic sites causes a shift in the affinities of the sites so that they selectively prefer less hydrated, larger atomic radius ions such as K^+ or carbachol cations over Na^+ or H^+, for example, as predicted from the theory of Ling (43) and Eisenman (44) and *(b)* carbachol–salt binding can be reinforced by hydrophobic bonding and van der Waals interactions, it is reasonable to assume that carbachol cations have a decided competitive advantage over other cations in the environment with regard to reoccupying the vacated fixed anionic sites.

The proposal of Klotz (45), which implicates the presence of iceberg-like structured water on protein surfaces in the alteration of acidic pK values of ionic and ionogenic side-chain groups, lends additional insight into the mechanistic nature of carbamylcholine cation-induced cooperative changes in the fixed charge density. Structured tissue water is stabilized as water of hydrophobic hydration on nonpolar protein side-chain groups (44, 45) and peptide linkages (40). This structured water is responsible for increasing the acidic pK's of fixed ionogenic groups relative to their values in unstructured water (40); the presence of cationic quaternary ammonium groups, such as those found on carbachol, causes a disruption of the water structure (44, 47, 48) which, in turn, favors ionization of ionogenic groups.

The operation of a mechanism of this nature is possibly a contributing factor to the sudden unmasking of anionic corneal surface sites which delineate the various discrete carbachol concentration ranges in Fig. 4. The formation and disruption of structured water occur in an abrupt cooperative manner (48), which could account for the observed precipitous changes in fixed charge density which are suggestive of the involvement of a cooperative mechanism (49).

Construction of Carbachol–Tissue Sorption Isotherms from Bioelectrometric Data—Although the fixed charge density of the corneal surface at the pH of the carbachol solutions is anionic, the observable anionic fixed charge density is less than the actual density of anionic binding sites due to a partial masking of these sites by electrically compensating, fixed cationic sites. All anionic sites are postulated as being capable of participation in the drug–tissue interactions. If the binding of α cations gives rise to a change of one unit of fixed charge density, the interaction of cationic solutes with the corneal surface may be described by the equilibrium presented in Scheme I:

$$S^- + \alpha c^+ \rightleftharpoons Sc_\alpha$$

Scheme I

where α is an apparent stoichiometric coefficient. For direct electrostatic salt binding of cations to fixed anionic sites, α would have a value of unity. In cases of interactions that indirectly result in an altered fixed charge density, α may have almost any value and in fact can vary as a function of the concentration of the applied interacting solute.

Table III—Binding Data for Interaction of Carbachol in pH 6.95 Buffer with the Corneal Surface of Rabbits

Carbachol Solution Molarity	Maximum Number of Binding Sites	Stoichiometric Coefficient, α	Apparent Association Constant, K
$0–2.74 \times 10^{-2}$	275[a]	0.87	0.80
$3.8 \times 10^{-2} – 5.5 \times 10^{-2}$		3.2	5×10^2
$8.8 \times 10^{-2} – 1.11 \times 10^{-1}$	277[b]	4.7	3×10^4
$1.25 \times 10^{-1} – 1.73 \times 10^{-1}$	425[c]	1.9	36

[a] Δf_{∞_1} in milliequivalents per liter. [b] Δf_{∞_2}. [c] Δf_{∞_3}.

It can be assumed for the present that an unknown number, α, of carbamylcholine cations, c^+, reacting with each anionic binding site, S^-, to form a complex, Sc_α, is responsible for the reduction of 1 equivalent of fixed charge density; $1/\alpha$ equivalents of negative fixed charge are neutralized for each equivalent of cation bound to form the complex. In other words, an observed change in fixed charge density, Δf, in the presence and absence of the cationic sorptate, when equal to 1 equivalent, is tantamount to the interaction of α moles of the cation. The relationship between free anionic binding sites, S^-, and the fixed charge density of the surface, f, is implicit in the value of α.

The affinity of the drug–tissue interaction may be described by an apparent association constant, K, as given by Eq. 1:

$$K = \frac{Sc_\alpha}{(c^+)_c{}^\alpha (S^-)} \qquad \text{(Eq. 1)}$$

where $(c^+)_c$ is the concentration of interacting cation in the colloid surface phase.

Rossotti and Rossotti (51) indicated that any property that varies with the degree of complex formation may be used to determine its extent. In the present case, observed changes in the fixed charge density represent experimentally known quantities which can be used for this purpose. Equation 1 can be rewritten fully in terms of experimental quantities to yield:

$$K = \frac{\Delta f}{[r^z(c^+)_{aq}]^\alpha(\Delta f_\infty - \Delta f)} \qquad \text{(Eq. 2)}$$

In Eq. 2, the observed change in fixed charge density at equilibrium, Δf, represents the concentration of the complex. The interacting cations in the applied solution distribute into the colloid surface phase in accordance with a Donnan equilibrium and must, therefore, be corrected by multiplication by r^z, where r is the Donnan ratio and z is the valence of the interacting cations. In the present treatment, the value of z is 1 for the carbamylcholine cation. The number of unaffected binding sites at equilibrium is the difference between the total number of anionic sites capable of interaction, Δf_∞, and the number of affected sites, Δf.

Equation 2 may be written in the forms given by Eqs. 3 and 4 for applicability to each of the three carbachol concentration regions in Fig. 4 preceding or following precipitous changes of Δf, which, as previously discussed, are postulated as being due to a cooperative, all-or-none unmasking of anionic sites:

$$K = \frac{\Delta f + f_1}{[r^z(c^+)_{aq}]^\alpha[\Delta f_{\infty_2} - (\Delta f + f_1)]} \qquad \text{(Eq. 3)}$$

$$K = \frac{\Delta f + f_1 + f_2}{[r^z(c^+)_{aq}]^\alpha[\Delta f_{\infty_3} - (\Delta f + f_1 + f_2)]} \qquad \text{(Eq. 4)}$$

In Eqs. 2–4 Δf_∞, Δf_{∞_2}, and Δf_{∞_3} are extrapolated total numbers of anionic sites for each of the three regions; f_1 and f_2 represent the changes in Δf between regions one and two and between regions two and three, respectively. The total density of anionic fixed charge that has been influenced up to a given carbachol concentration is given by Δf, $(\Delta f + f_1)$, and $(\Delta f + f_1 + f_2)$ for the concentration regions of 0–0.055, 0.088–0.111, and 0.125–0.173 M, respectively. Equations 2–4 are, in principle, equivalent if the newly

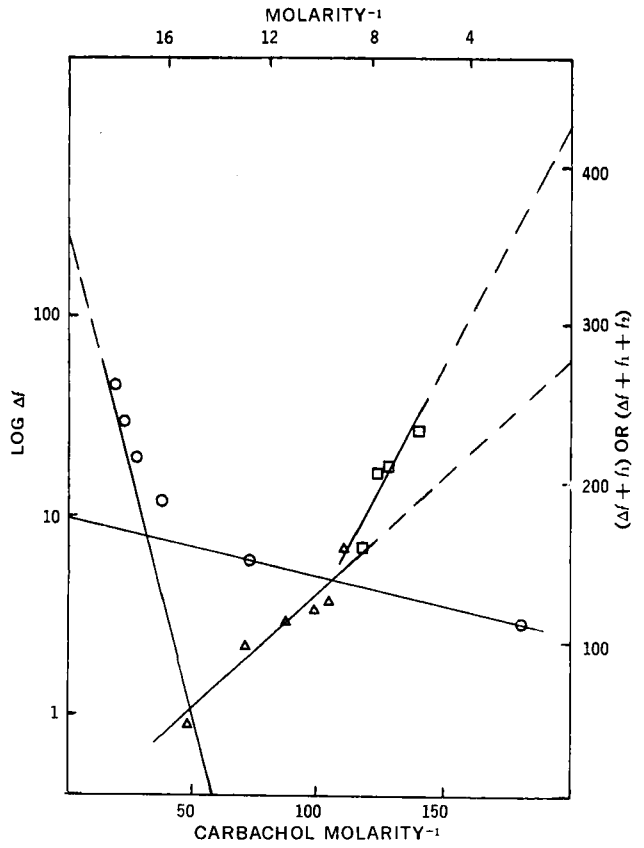

Figure 5—*Graphical determination of the maximum number of binding sites, Δf_∞, on the rabbit corneal surface which bind carbamylcholine cations at pH 6.95. The Δf_∞ values are determined by extrapolating the change in fixed charge density to infinite carbachol concentration for each of the binding regions shown corresponding to 0–5.5 × 10⁻² M (○), 8.8 × 10⁻²–1.11 × 10⁻² M (△), and 1.25 × 10⁻²–1.73 × 10⁻⁴ M (□) carbachol.*

created anionic binding sites are considered as being included in the total of cation-affected sites up to any given concentration.

Generally, some form of Eq. 2 suffices for the treatment of most solute–tissue interaction data. The observation that precipitous changes in Δf do occur attests to the verity of the expectation that heterogeneous tissue sites are characterized by differing interaction parameters. If this were not the case, the binding would be describable by a monotonic Δf *versus* carbachol concentration function indicating identical independent binding sites which, when transformed into a sorption isotherm, would be Langmuirian in appearance.

Values of Δf_∞ were obtained graphically (Fig. 5) by linear extrapolations to ordinate values corresponding to infinite concentrations of interacting carbachol. One plot of Δf *versus* the reciprocal of carbachol concentration was nonlinear, having a shape resembling an exponential decay. This appearance suggested its resolution into a sum of contributing exponentials, using the familiar peeling-off technique (52) and obtaining the sum of the least-squares values of the intercepts of semilogarithmic plots of each contributing exponential component. The results of the application of this technique are illustrated in Fig. 5, where the sum of the ordinal intercepts gives the apparent total number of available binding sites corresponding to an infinite concentration of carbachol for the 0–0.055 *M* region. Table III lists the values of total available sites appropriate for the three discrete binding regions.

Equation 5 is a linearized, logarithmic form of Eq. 2. Values of α and K may be determined from the slopes and intercepts of corresponding log–log plots of Eq. 5:

$$\log\left[\frac{\Delta f}{\Delta f_\infty - \Delta f}\right] = \log K + \alpha \log\left[r^z(c^+)_{aq}\right] \quad \text{(Eq. 5)}$$

The values of all terms appearing in Eq. 5 except α, K, and Δf_∞ are known from experimental procedures. As previously mentioned, the apparent stoichiometric coefficient, α (as well as the affinity constant, K), may be different in each concentration region as well as being concentration dependent within each region due to heterogeneity of binding sites and a varying reactivity of the sites that can be dependent upon the extent of their occupation. When this is fully the case, α and K may be approximated at each adsorptate concentration from the slope and intercept of a tangent line drawn to the curve at each abscissal concentration value. The accuracy of such a procedure could, when necessary, be enhanced by curvilinear regression fitting of the log–log plot to an empirical equation and differentiating the equation to obtain the slopes at each concentration. However, the evaluation of K and α would still remain uncertain due to the error generally characteristic of first derivative estimations.

Fortunately, it has been the experience of the authors that such log–log plots are either linear or exhibit two or more regions of linearity in which α and K are relatively constant. When this is the case, a plot of log $[\Delta f/(\Delta f_\infty - \Delta f)]$ *versus* log $[r^z(c^+)_{aq}]$ provides α as the slope of the line and log K as the intercept on the ordinate at $[r^z(c^+)_{aq}] = 1$. Equations 3 and 4 obviously can be linearized similarly to Eq. 2 and values of α and K can be evaluated.

Plots of Eqs. 2–4 for the present study are exemplified in Fig. 7. The plot for the lowest concentration region reveals two distinct straight lines, indicating a heterogeneity of binding sites within this region, with each type of site having its own α and K values. The values of α, as calculated from the least-squares slopes of the lines, are listed in Table III. The value of α in the carbachol concentration region of 0.088–0.111 *M* suggests that four to five carbamylcholine cations, when bound to the cornea, give rise to a change of approximately one unit of fixed charge density. This result is reasonable if one postulates a release of nondrug cations every time a drug cation is bound. The number of equivalents of bound cation that causes an integral value can be interpreted as representing a weighted average of integral values which must necessarily occur on a microscopic scale. The values of the association constant, K, for each concentration region are also listed in Table III. As anticipated, these values differ along with the α values in each concentration region. In the lowest concentration region,

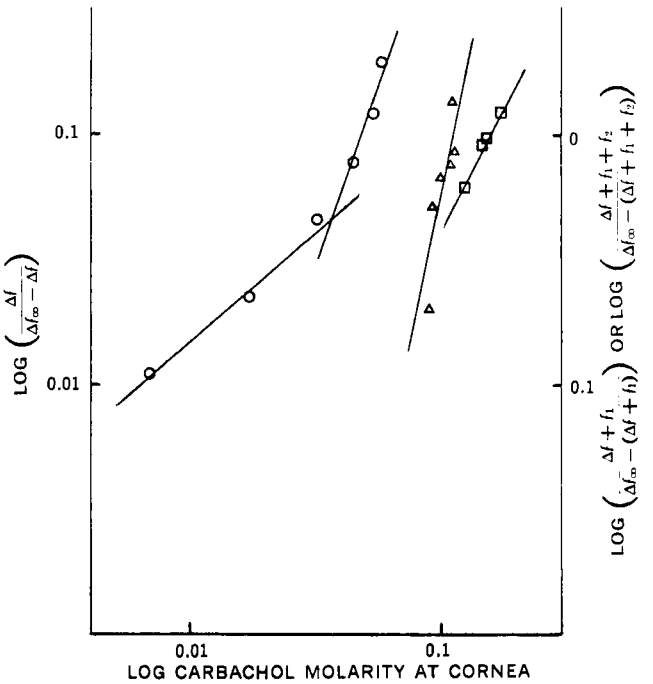

Figure 6—*Bjerrum-type plots of electrometric results of carbachol interaction with rabbit cornea. The three plots correspond to the carbachol concentration regions of 0–2.74 × 10⁻² M (○), 8.8 × 10⁻²–5.5 × 10⁻² M (△), and 1.25 × 10⁻²–1.73 × 10⁻² M (□). The ordinate scale on the right side is used for the plots corresponding to the latter two regions.*

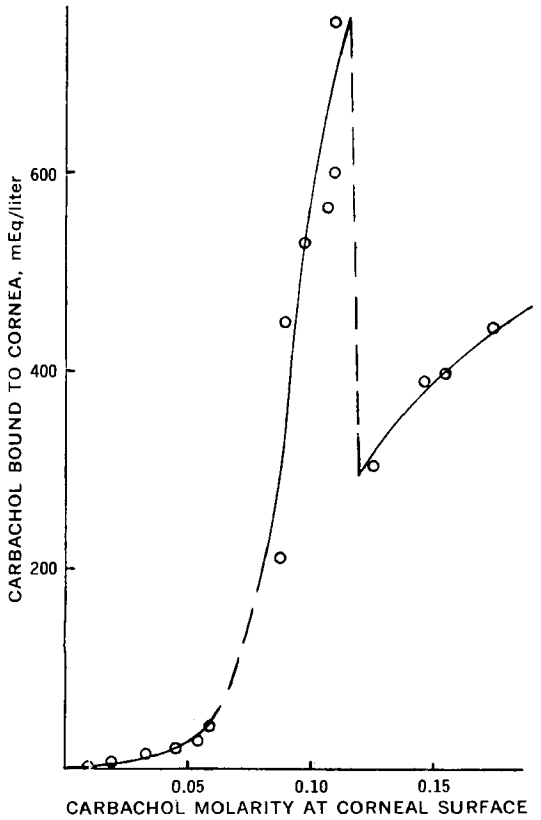

Figure 7—*Sorption isotherm describing the binding of carbamylcholine cations to the corneal surface of rabbits at pH 6.95. The dashed portions of the curve represent the intervals between the three binding regions which are defined by abrupt changes in fixed charge density.*

there are evidently two types of sites with different K values.

Having determined α values from the log–log plots, the equivalents of corneal surface-bound carbachol can be obtained by multiplying Δf [or $(\Delta f + f_1)$ or $(\Delta f + f_1 + f_2)$] by corresponding values of α. From Eqs. 2–4:

$$\left.\begin{aligned} &\alpha(Sc_a) = \alpha\Delta f \\ &\alpha(\Delta f + f_1) \\ &\alpha(\Delta f + f_1 + f_2) \end{aligned}\right\} = \text{cornea bound carbachol} \qquad \text{(Eq. 6)}$$

An adsorption isotherm may be constructed by plotting the quantity of bound carbachol as a function of the carbachol concentration in the corneal surface phase, *i.e.*, $[r^2(c^+)_{aq}]$. The cooperative nature of the drug–tissue interaction is again apparent from the shape of the isotherm in Fig. 7. Inspection of Fig. 7 reveals an unusual effect. When accepting the method by which they were attained, the results in Fig. 7 indicate that the interaction of carbachol decreased in the 0.125–0.173 M region relative to the 0.088–0.111 M region. This behavior may be rationalized by postulating that in the transition between these two concentration regions, in which new anionic sites are unmasked due to a release of cations, the released cations include carbachol; vacated sites subsequently become reoccupied by carbachol when its concentration is increased.

The decrease in the association constant for carbachol binding from a value of 3×10^4 to 36 (Table III) indicates a large decrease in affinity for carbachol interaction which underlies the desorption of carbachol from the tissue surface in the transition between the second and third concentration regions. Since there is no apparent similar discontinuity between the first and second concentration regions in Fig. 7, it can be assumed that the abrupt drop in charge density occurring between these regions (Fig. 4) reflects a release of nondrug cations, Na^+, K^+, *etc.*, from the tissue surface rather than carbamylcholine cations. Table III shows that the carbachol association constant is appreciably greater for the second region compared to the first region, indicating an enhancement of drug cation binding in the second region. The opposite occurs in the third region.

Carbachol–Corneal Surface Interaction and Drug Bioavailability Implications—Since carbachol must penetrate into, and migrate through, the cornea, it seems reasonable to expect that the size of the reservoir of drug sorbed onto the corneal surface will affect the amount of drug reaching the biophase. The amount of bound drug on the corneal surface is dependent on the availability of binding sites and the affinity of the drug for the surface; weakly bound drug is easily washed off in the lacrimal fluid. In the preceding discussion, it was postulated that drug–tissue affinity is reflected in the observed changes in the fixed charge density of the drug-treated tissue surface. A correlation may be expected between tissue-bound drug and the amounts of drug and the time they are available to exert a local pharmacological response.

The duration of the miotic response provides a measure of such drug bioavailability; the response duration is defined as the time required for the pupil diameter to return to normal. In Fig. 8, the response duration is plotted as a function of the concentration of topically administered carbachol solutions. It is evident from the figure that the duration first increases monotonically with increasing carbachol concentration; it then decreases and eventually increases again as the concentration is further raised. The sharp decrease in duration is approximately in the same concentration region where an abrupt drop in charge density (Fig. 4) and bound carbachol (Fig. 7) occurs. This abrupt change was attributed to desorption of carbamylcholine cations from tissue binding sites. It appears that the bioavailability of topically administered carbachol is dependent on the extent of interaction of carbachol with the corneal surface and can be enhanced by modifying the drug dosage form so as to increase this interaction.

In a subsequent paper of this series, it will be proposed that the adjuvant, benzalkonium chloride, enhances the bioavailability of carbachol by affecting carbamylcholine binding sites on the corneal surface. In the first paper of this series, it was proposed that this

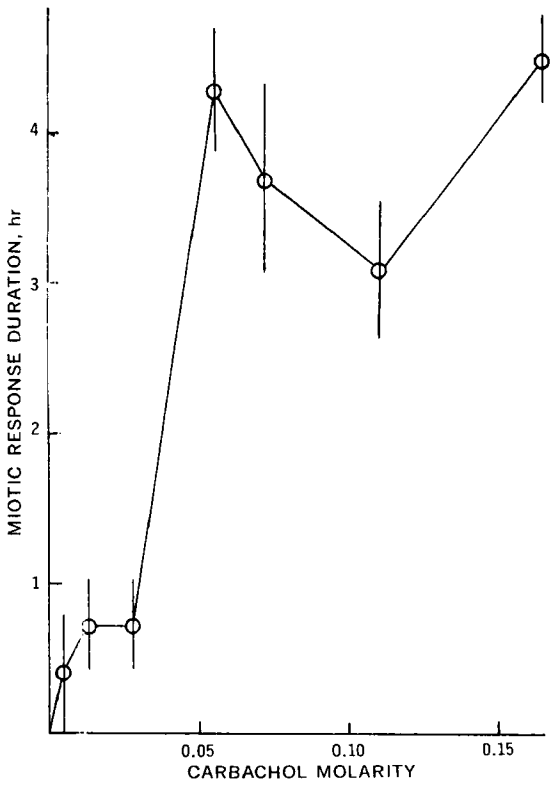

Figure 8—*Dependency of the duration of carbachol-induced miotic response activity in rabbits on the carbachol concentration in topically administered, pH 6.95, ophthalmic solutions. Each point represents the average of a minimum of four replications. The standard deviations are shown for each point.*

adjuvant also functions in facilitating the transport of carbachol through the cornea to the aqueous humor by inducing the release of bound carbamylcholine from tissue binding sites throughout the cornea (1).

As was the case in Fig. 7, no drop in response duration in the lowest carbachol concentration region is evident in Fig. 8, which supports the contention that the first abrupt drop in charge density in Fig. 4 reflects a release of nondrug cations from the corneal surface. The small initial increase in duration at very low carbachol concentrations could conceivably be a result of the low affinity of drug cations for surface sites as predicted by the small drug–tissue association constant (Table III). For these concentrations, one can speculate that the binding of carbamylcholine cations to the corneal surface also augments movement of drug cations across the cornea by creating a more favorable electrical gradient.

Iontophoresis, a procedure used to facilitate the transcorneal passage of anionic and cationic drugs (53), emphasizes, in conjunction with other evidence, the electrostatic and presumably electrochemical factors that influence passage of ophthalmic drug ions from the epithelial tear interface to the aqueous humor. Concomitant conformational changes in biocolloids resulting in morphological changes in the cells constituting the epithelial barrier must also be considered as related factors that could affect the transcorneal transport of carbachol. For example, Green and Tonjun (54) reported that an electron microscopically observed widening of intercellular spaces in the corneal epithelium results from treatment with surface-active quaternary ammonium compounds. If this occurs *in vivo, i.e.,* it is not merely a consequence of the harsh treatment of the excised corneal tissue subjected to dehydration and osmium fixation in the process of making electron micrographs, it is likely that submolecular phenomena, such as those presently described, underlie the widening process (31, 41) and, by this mechanism, could also contribute to enhancing transcorneal drug passage.

SUMMARY

The present study was directed to an elucidation of the submolecular interaction of the ophthalmic drug carbachol with the corneal surface of rabbits. An *in vivo* bioelectrometric method, which permitted determination of the fixed charge density of the corneal surface in response to varying the carbachol concentration of topically administered solutions, was implemented.

The reversible pH–titration curve of the cornea illustrates the amphoteric, predominantly acidic, nature of the tissue surface and is due to the various protein, lipid, nucleic acid, and mucopolysaccharide constituents of the corneal surface. The interaction of carbamylcholine cations with the corneal surface is a complex phenomenon which apparently involves cooperative, all-or-none changes in association affinities of fixed anionogenic groups on the surface. The mechanism of the interaction is explainable in terms of an inductive alteration of cation binding site affinities as a consequence of the binding of carbachol cations to vicinal cardinal sites. Corresponding miotic results indicate that the bioavailability of the drug is dependent on the extent of the drug–tissue interaction and reflects alterations in the values of the parameters characterizing the interaction.

REFERENCES

(1) V. F. Smolen, J. M. Clevenger, E. J. Williams, and M. W. Bergdolt, *J. Pharm. Sci.*, **62,** 958(1973).

(2) C. S. O'Brien and K. C. Swan, *Trans. Amer. Ophthalmol. Soc.*, **39,** 175(1941).

(3) V. F. Smolen and F. P. Siegel, *J. Pharm. Sci.*, **57,** 378(1968).

(4) V. F. Smolen, D. E. Snyder, and R. J. Erb, *ibid.*, **59,** 1093(1970).

(5) R. I. Poust and V. F. Smolen, *ibid.*, **59,** 1461(1970).

(6) V. F. Smolen and R. I. Poust, *ibid.*, **60,** 1745(1971).

(7) V. F. Smolen and L. D. Grimwood, *J. Colloid Interface Sci.*, **36,** 308(1971).

(8) V. F. Smolen and E. J. Williams, *J. Pharm. Sci.*, **61,** 921(1972).

(9) V. F. Smolen, *Can. J. Pharm. Sci.*, **7,** 7(1972).

(10) C. S. Park, M.S. thesis, Purdue University, West Lafayette, Ind., 1972.

(11) R. I. Poust, Ph.D. thesis, Purdue University, West Lafayette, Ind., 1971.

(12) V. F. Smolen, *J. Pharm. Sci.*, **60,** 354(1971).

(13) V. F. Smolen and R. D. Schoenwald, *ibid.*, **60,** 96(1971).

(14) R. D. Schoenwald and V. F. Smolen, *ibid.*, **60,** 1039(1971).

(15) V. F. Smolen, *Amer. J. Pharm. Educ.*, **33,** 381(1969).

(16) D. M. Maurice, *Exp. Eye Res.*, **6,** 138(1967).

(17) R. W. Modrell and A. M. Potts, *Amer. J. Ophthalmol.*, **48,** 834(1959).

(18) D. M. Maurice, in "The Eye, Vegetative Physiology and Biochemistry," vol. 1, H. Davson, Ed., Academic, New York, N.Y., 1969, pp. 554, 555.

(19) K. Green, *Amer. J. Physiol.*, **209,** 1311(1965).

(20) V. F. Smolen and R. I. Poust, *J. Pharm. Sci.*, **61,** 1101(1972).

(21) J. S. Friedenwald, W. F. Hughes, and H. Herrmann, *Arch. Ophthalmol.*, **31,** 279(1944).

(22) R. B. Martin, "Introduction to Biophysical Chemistry," McGraw-Hill, New York, N.Y., 1964, p. 79.

(23) P. Alexander and R. F. Hudson, "Wool—Its Chemistry and Physics," Reinhold, New York, N.Y., 1954, p. 181.

(24) G. N. Ling, *Int. Rev. Cytol.*, **26,** 1(1969).

(25) V. F. Smolen, *Ann. N. Y. Acad. Sci.*, **204,** 323(1973).

(26) J. Monod, J. P. Changeux, and F. Jacob, in "Allosteric Regulation," M. Takashige, Ed., University Park Press, Baltimore, Md., 1971, pp. 3–26.

(27) F. W. Cope, *Advan. Biol. Med. Phys.*, **13,** 1(1970).

(28) M. B. Engel, N. R. Joseph, D. M. Laskin, and H. R. Catchpole, *Amer. J. Physiol.*, **201,** 621(1961).

(29) A. Szent-Gyorgi, "Bioelectronics," Academic, New York, N.Y., 1968, pp. 1–80.

(30) R. Dalmadian, *Biophys. J.*, **11,** 773(1971).

(31) J. Monod, J. P. Changeux, and F. Jacob, *J. Mol. Biol.*, **6,** 306(1963).

(32) G. N. Ling, *Biopolymers,* Symposia No. 1 (1964), pp. 91–166.

(33) M. G. Evans and J. Gergely, *Biochim. Biophys. Acta,* **3,** 188(1949).

(34) P. Alexander and R. F. Hudson, "Wool—Its Chemistry and Physics," Reinhold, New York, N.Y., 1954, pp. 181–244.

(35) C. Tanford, *Advan. Protein Chem.*, **17,** 70(1962).

(36) H. P. Ludgren, *Text. Res. J.*, **15,** 335(1945).

(37) I. L. Reisen and J. Gulati, *Science,* **176,** 1137(1972).

(38) J. Gulati and I. L. Reisen, *ibid.*, **176,** 1141(1972).

(39) J. Steinhardt and E. M. Zaiser, *Advan. Protein Chem.*, **10,** 160(1955).

(40) H. N. Glassman, *Ann. N. Y. Acad. Sci.*, **53,** 91(1950).

(41) N. R. Joseph, H. P. Catchpole, D. M. Laskin, and M. B. Engel, *Arch. Biochem. Biophys.*, **84,** 224(1959).

(42) G. N. Ling, *Fed. Proc.*, **25,** 958(1966).

(43) G. N. Ling, "A Physical Theory of the Living State," Blaisdell, New York, N.Y., 1962, pp. 518–521.

(44) G. Eisenman, in "Symposium on Membrane Transport and Metabolism," A. Kleinzeller, Ed., Publishing House of Czechoslovakia Academy of Science, Prague, Czechoslovakia, 1961, pp. 163–179.

(45) I. M. Klotz, *Science,* **128,** 815(1958).

(46) V. F. Smolen and D. E. Hagman, *J. Colloid Interface Sci.*, **42,** 70(1973).

(47) G. N. Ling, *Int. Rev. Cytol.*, **26,** 1(1969).

(48) W.-Y. Wen, in "Water and Aqueous Solutions," R. A. Horne, Ed., Wiley-Interscience, New York, N.Y., 1972, pp. 613–661.

(49) H. A. Scheraga, *Ann. N. Y. Acad. Sci.*, **125,** 253(1965).

(50) G. N. Ling, *ibid.*, **125,** 663(1965).

(51) F. J. C. Rossotti and H. Rossotti, "The Determination of Stability Constants," McGraw-Hill, New York, N.Y., 1961.

(52) D. S. Riggs, "Mathematical Approach to Physicological Problems," Williams & Wilkins, Baltimore, Md., 1963, pp. 120–168.

(53) W. H. Havener, in "Ocular Pharmacology," C. V. Mosby, St. Louis, Mo., 1970, p. 204.

(54) K. Green and A. Tonjun, *Amer. J. Ophthalmol.*, **72,** 897(1971).

ACKNOWLEDGMENTS AND ADDRESSES

Received from the *Biophysical Pharmaceutics Area of the Department of Industrial and Physical Pharmacy, School of Pharmacy and Pharmacal Sciences, Purdue University, West Lafayette, IN 47907*

Presented in part to the Symposium on Drug-Biomolecule Interactions, APhA Academy of Pharmaceutical Sciences, fall meeting, Chicago, Ill., November 1972.

Abstracted in part from a thesis submitted by C. S. Park to Purdue University in partial fulfillment of the Master of Science degree requirements.

Supported in part by Alcon Laboratories, Inc., Fort Worth, Tex.

This paper is Part II in the series "Bioavailability of Ophthalmic Carbachol."

[x] To whom inquiries should be directed.

Drug–Biomolecule Interactions: Drug Toxicity and Vitamin Coenzyme Depletion

JOHN P. BEDERKA, Jr. [*x], DANIS DAVITIYANANDA [‡], MIKEL L. MOSES [*], and NASIM AHMAD [*§]

Abstract □ Thirteen pyridine compounds, phenylbutazone, and three salicylates were studied for their effects upon the turnover of 7-^{14}C-nicotinamide dinucleotides in the mouse. The compounds were administered at equitoxic doses (LD_{25}) to 7-^{14}C-nicotinic acid- (niacin) pretreated mice, and the induced excretion of urinary-^{14}C was analyzed in terms of total ^{14}C and percentage of total ^{14}C as known metabolites of nicotinic acid. Of the 17 compounds, 12 afforded significant alterations in the total ^{14}C excreted and five of these caused alterations in the disposition of the 7-^{14}C-nicotinamide endogenously liberated from the 7-^{14}C-nicotinamide adenine dinucleotide pool. Comparative depletions of ^{14}C from brain, lungs, liver, and kidneys were studied with 10 of the pyridine compounds. Several tissues were found to be the sources of the urinary-^{14}C, with the lungs being the most accessible source. Some compounds had effects at doses less than the LD_{25}'s, as shown by increased hexobarbital sleeping time in acute experiments with rats. These pyridine compounds were initially considered to act at the level of the nicotinamide dinucleotides in the normal biosynthetic pathway (nicotinic acid site) and/or at the level of glycohydrolase (nicotinamide site). In view of the inclusion of nicotinic acid, nicotinamide, salicylic acid, and phenylbutazone in this correlation between toxicity and 7-^{14}C-nicotinamide mobilization, it is not necessary that the formation of compounds analogous to the nicotinamide dinucleotides plays a significant role in the toxic manifestations of the nicotinamide analogs. The displacement of 7-^{14}C-nicotinamide dinucleotides from their corresponding apoenzymes with subsequent metabolism of the dinucleotides could explain the noted increased 7-^{14}C-nicotinamide dinucleotide turnover and depletion which led to the toxic effects.

Keyphrases □ Coenzyme depletion—effects of 17 compounds, motor activity, sleeping time, toxicity, therapeutic effects, coenzyme binding site □ Toxicity—pyridine compounds, salicylates, phenylbutazone, nicotinic acid site, nicotinamide site, coenzyme binding site □ Metabolism—nicotinamide, coenzymes, nicotinamide dinucleotides, apoenzymes □ Drug–biomolecule interactions—drug toxicity and vitamin coenzyme depletion, symposium □ Interactions—drugs with biomolecules, symposium

Since initial toxicity studies (1, 2), McDaniel *et al.* (3) described niacin and seemingly anomalous antiniacin or toxic effects of 3-acetylpyridine and several attempts have been made to reconcile such disparities. Thus, antiniacin properties were considered in compounds related to nicotinic acid (niacin) and nicotinamide (niacinamide) (4–6). Since these studies with nicotinamide and some possible antimetabolites, attention has been focused on the nicotinamide dinucleotides[1] (NAD and NADP). The production of analogs and/or alterations in the concentrations of these dinucleotides have been considered as possible explanations of the antiniacin effects of 3-acetylpyridine (5–9) and of 6-aminonicotinamide (10).

It has been reported that nicotinamide administration results in increased levels of liver NAD, with maximal increases at 8–12 hr after the administration of 250 mg/kg ip to the mouse (11) and 1 g/kg ip to the rat (12). The latter study showed a relationship among the increased nicotinamide (23-fold), nicotinic acid (65-fold), and NAD (11-fold) levels in the liver after nicotinamide administration. This induced synthesis is in accord with the normal biosynthetic pathway (Scheme I), wherein the *in vivo* hydrolysis of nicotinamide would furnish the nicotinic acid.

Moreover, compounds other than nicotinic acid and nicotinamide have been reported to increase liver NAD levels. Kaplan *et al.* (11) showed that the administration of 3-methylpyridine (β-picoline) afforded a higher liver NAD level and more rapid rise to maximal effect than did nicotinamide. This increase could possibly be explained as a consequence of the continuous *in vivo* oxidation of 3-methylpyridine to nicotinic acid, with resultant NAD biosynthesis. Alternatively, and perhaps concomitantly, the 3-methylpyridine could cause a general tissue depletion of NAD whose mobilization could lead to the liver levels of NAD described.

Nicotinamide and related substances lend themselves readily to studies relating biological effect and biochemical change, since the normal biotransformations of nicotinamide have been intimately defined in regard to NAD biosynthesis (13) and to nicotinamide

[1] The phrase nicotinamide dinucleotides will include the oxidized [NAD (nicotinamide adenine dinucleotide) and NADP (nicotinamide adenine dinucleotide phosphate)] and corresponding reduced forms (NADH and NADPH) since quantitative assessments of the amounts of the individual substances have not been performed.